Optics Communications

Implementation of a Fiber-Based Resonant Beam System for Multiuser Optical Wireless Information and Power Transfer

--Manuscript Draft--

Manuscript Number:	XY-083R1
Article Type:	Research Paper
Keywords:	Resonant beam; free-space optics; Energy Harvesting; optical wireless information and power transfer
Corresponding Author:	Hsu-Chih Cheng National Formosa University Yunlin, TAIWAN
First Author:	Chun-Ming Huang
Order of Authors:	Chun-Ming Huang
	Eddy Wijanto
	Shin-Pin Tseng
	Yu-Tang Luo
	Yu-Hao Liu
	Hui-Chi Lin
	Hsu-Chih Cheng
Abstract:	A fiber-based resonant beam system is proposed for a simultaneous optical wireless information and power transfer (OWIPT) system. A fiber Bragg grating and an optical circulator are used to achieve simultaneous wireless optical communication and power transmission. In the receiver subsystem, a communication and energy harvesting circuit is employed to separate alternating current (AC) and direct current (DC) outputs. The AC output is used for information transmission, and the DC output is used for power transfer. We conducted experiments to test the built-in safety mechanism to verify whether the resonant beam stops immediately if any obstacle obstructs the line of sight of the system. The proposed architecture can be constructed for indoor and outdoor multiuser applications. The results demonstrated that the proposed fiber-based resonant beam system can be implemented successfully for simultaneous OWIPT.
Suggested Reviewers:	
Response to Reviewers:	Comments from Reviewer 1 and Responses We appreciate your constructive comments and suggestions, which have helped refine this manuscript. We have revised the manuscript according to your comments, and our responses are presented as follows. Comment 1: The logic and necessity in application level of this fiber-based resonant beam system for wireless information and power transfer to 5g and FSOC area is much to forced. So, the introduction part should be adjusted. Response: Thank you for your suggestion. On the basis of your suggestion, we have revised the introduction. In particular, we have added the following explanations to the introduction of the revised manuscript (page 1-2): “Smartphones and other mobile devices have become an inseparable part of today’s daily lives. Throughout the day, most people are sending messages and emails, making voice or video calls, posting on social networks, and playing online games. The increasing usage of mobile devices also increases the average daily power consumption from a typical device battery. In addition, fifth-generation (5G) mobile technologies are projected to support massive amounts of data at high bit rates with minimal delay [1]. This feature of 5G technologies will stimulate many new applications with sophisticated multimedia signal processing, which will increase battery usage. Furthermore, rapid development of the Internet of things (IoT) is driving the demand for

high-bit-rate and low-latency wireless information transfer. One challenge of the IoT is that typical IoT devices are designed to operate from battery power and have limited energy. Some IoT devices cannot have their batteries replaced. In addition, frequent battery charging for mobile devices by using conventional wired mechanisms tends to obstruct user mobility. In such cases, wireless power transmission (WPT) can be a solution. Free-space optics (FSO) is a promising WPT method [2] that provides high data rates, is immune to radio frequency (RF) interference, does not require licensing, provides a highly secure communication link, is relatively fast, and can be deployed easily. The only substantial consideration for FSO is line of sight (LOS) between the transmitter and receiver."
Comment 2:
In Fig.4 Multiuser fiber-based OWIPT architecture is provided. In the transmitter end, this paper mentioned FBGs with two different wavelengths (λ1 and λ2), but without any information about FBGs equipment type and device model, and without the principle that how two different wavelengths share the same information channel. Please give more information about the FBGs in figure mode, such as the architecture and principle of the FBGs with more than one wavelengths.
Response:
As per your suggestion, we have added the type of FBG along with the device supplier. First, in the multiuser experiments, we used two uniform FBG devices with different central wavelengths at 1546.85 nm and 1549.7 nm; these are denoted as λ1 and λ2, respectively. Then FBG devices were manufactured by 3L Technologies Inc., Taiwan. Second, we have added the following text to the proposed FBG-based OWIPT system of the revised manuscript (page 9):
"In the transmitter, two FBGs (λ1 and λ2) reflect different users' optical signals. Because the transmitter is paired with one or more receivers, each user utilizes one pair of FBGs with the same wavelength for resonating. In the experiment, two pairs of FBGs with different wavelengths (λ1 and λ2) were used for user #1 and user #2, respectively. In the receiver, an FBG of the corresponding wavelength is used to split the signals across users. The optical signals are divided into two branches. The first branch is used to reflect the signals back into the circulator, thus completing the resonant beam scheme. The second branch is used for information and power harvesting. The reflected optical signal enters the EOM and is modulated using a signal generator for information transmission. In this experiment, the information sent from the message part to the EOM is a broadcast message from one transmitter to two receivers."

Third, we have added the manufacturer of FBG devices to the experimental results of the revised manuscript.
Finally, we have added the following discussion to the experimental results of the revised manuscript:
"When the collimator at the transmitter and the collimator at receiver #2 were aligned, the wavelength of the resonant beam changed from 1546.83 nm (λ1) to 1549.7 nm (λ2). Furthermore, the message modulated at the central wavelength of λ2 from the transmitter could be reconstructed by the FBG of receiver #2 operating at the corresponding wavelength of λ2."

Comments from Reviewer 2 and Responses

We appreciate your valuable comments, which have assisted us to refine this manuscript. We have revised the manuscript according to your comments, and our responses are presented as follows.
Comment 1:
The author can explain figure 1 in more detail.
Response:
As per your suggestion, we have added the following explanations for Figure 1 to the

	introduction of the revised manuscript (page 3-4): “Figure 1 illustrates the features of an OWIPT system based on a resonant beam. In a typical WPT or wireless information transmission (WIT) system that utilizes a laser as a source, a high-intensity laser beam must be emitted from a specific distance to the receiver end. A laser-based WPT or WIT usually faces the challenges of mobility and safety; therefore, they typically are used only for low-power and short-distance applications [5]. To overcome the limitations of typical laser-based WPT or WIT systems, the OWIPT system in this study enabled high-power beam transmission through a laser resonant cavity. This RBC-based OWIPT system utilized a resonant beam to transmit watt-level power over meter-level ranges and to multiple mobile devices concurrently. In the case that any obstacle blocks the beam, the resonant beam path stops the resonance mechanism immediately. When any obstacle is in the transmission path, diffraction loss in the cavity increases. Then, if the diffraction loss becomes larger than the system gain produced by the gain medium, the resonance terminates instantly. Conversely, when the obstacle moves out of the transmission path, the loss becomes smaller than the gain factor; therefore, the resonance is immediately reconstituted.” Comment 2: Figure 5 and Figure 6 can be clearer. The words are too small, and B image in the Figure 5 can not be seen clearly. It is recommended to draw 5 with different color lines (do not use black lines). Response: Because Figures 5 and 6 were produced by an optical spectrum analyzer, the color lines cannot be changed. However, we have added some additional marks for the wavelength and optical power levels in the Figures 5(a) and 6(a). Conversely, Figures 5(b) and 6(b) were unchanged because they are only noise-level spectra. Comment 3: The author's English expression ability needs to be improved. It is recommended that more conjunctions be used to make the sentence more smooth when comparing the two pictures. Response: Thank you for reviewing our manuscript thoroughly. The revised manuscript has been edited for proper English grammar, word usage, and overall style by a native English-speaking academic editor. Furthermore, we have added suitable conjunctions in the description of each picture.

Dear Editor,

We have revised the manuscript entitled as “Implementation of a Fiber-Based Resonant Beam System for Multiuser Optical Wireless Information and Power Transfer”, paper number XY-083, in accordance with reviewers’ comments. Attached are the files of the responses to the reviewers’ comments and the revised manuscript with the changes having underline. The manuscript has been edited for proper English language, grammar, punctuation, spelling, and overall style by a native English-speaking academic editor.

Thank you very much for your attention and help. We’re looking forward to hearing from you soon.

Sincerely yours,

Hsu-Chih Cheng, Ph.D.
Professor, Chairman
Department of Electro-Optical Engineering,
National Formosa University,
Yunlin, Taiwan ROC,
E-mail: chenghc@nfu.edu.tw

Comments from Reviewer 1 and Responses

We appreciate your constructive comments and suggestions, which have helped refine this manuscript. We have revised the manuscript according to your comments, and our responses are presented as follows.

Comment 1:

The logic and necessity in application level of this fiber-based resonant beam system for wireless information and power transfer to 5g and FSOC area is much to forced. So, the introduction part should be adjusted.

Response:

Thank you for your suggestion. On the basis of your suggestion, we have revised the introduction. In particular, we have added the following explanations to the introduction of the revised manuscript (page 1-2):

"Smartphones and other mobile devices have become an inseparable part of today's daily lives. Throughout the day, most people are sending messages and emails, making voice or video calls, posting on social networks, and playing online games. The increasing usage of mobile devices also increases the average daily power consumption from a typical device battery. In addition, fifth-generation (5G) mobile technologies are projected to support massive amounts of data at high bit rates with minimal delay [1]. This feature of 5G technologies will stimulate many new applications with sophisticated multimedia signal processing, which will increase battery usage.

Furthermore, rapid development of the Internet of things (IoT) is driving the demand for high-bit-rate and low-latency wireless information transfer. One challenge of the IoT is that typical IoT devices are designed to operate from battery power and have limited energy. Some IoT devices cannot have their batteries replaced. In addition, frequent battery charging for mobile devices by using conventional wired mechanisms tends to obstruct user mobility. In such cases, wireless power transmission (WPT) can be a solution. Free-space optics (FSO) is a promising WPT method [2] that provides high data rates, is immune to radio frequency (RF) interference, does not require licensing, provides a highly secure communication link, is relatively fast, and can be deployed easily. The only substantial consideration for FSO is line of sight (LOS) between the transmitter and receiver."

Comment 2:

In Fig.4 Multiuser fiber-based OWIPT architecture is provided. In the transmitter end, this paper mentioned FBGs with two different wavelengths (λ_1 and λ_2), but without any information about FBGs equipment type and device model, and without the principle that how two different wavelengths share

the same information channel. Please give more information about the FBGs in figure mode, such as the architecture and principle of the FBGs with more than one wavelengths.

Response:

As per your suggestion, we have added the type of FBG along with the device supplier. First, in the multiuser experiments, we used two uniform FBG devices with different central wavelengths at 1546.85 nm and 1549.7 nm; these are denoted as λ_1 and λ_2, respectively. Then FBG devices were manufactured by 3L Technologies Inc., Taiwan.

Second, we have added the following text to the proposed FBG-based OWIPT system of the revised manuscript (page 9):

"In the transmitter, two FBGs (λ_1 and λ_2) reflect different users' optical signals. Because the transmitter is paired with one or more receivers, each user utilizes one pair of FBGs with the same wavelength for resonating. In the experiment, two pairs of FBGs with different wavelengths (λ_1 and λ_2) were used for user #1 and user #2, respectively. In the receiver, an FBG of the corresponding wavelength is used to split the signals across users. The optical signals are divided into two branches. The first branch is used to reflect the signals back into the circulator, thus completing the resonant beam scheme. The second branch is used for information and power harvesting. The reflected optical signal enters the EOM and is modulated using a signal generator for information transmission. In this experiment, the information sent from the message part to the EOM is a broadcast message from one transmitter to two receivers."

Third, we have added the manufacturer of FBG devices to the experimental results of the revised manuscript.

Finally, we have added the following discussion to the experimental results of the revised manuscript:

"When the collimator at the transmitter and the collimator at receiver #2 were aligned, the wavelength of the resonant beam changed from 1546.83 nm (λ_1) to 1549.7 nm (λ_2). Furthermore, the message modulated at the central wavelength of λ_2 from the transmitter could be reconstructed by the FBG of receiver #2 operating at the corresponding wavelength of λ_2."

Comments from Reviewer 2 and Responses

We appreciate your valuable comments, which have assisted us to refine this manuscript. We have revised the manuscript according to your comments, and our responses are presented as follows.

Comment 1:

The author can explain figure 1 in more detail.

Response:

As per your suggestion, we have added the following explanations for Figure 1 to the introduction of the revised manuscript (page 3-4):

"Figure 1 illustrates the features of an OWIPT system based on a resonant beam. In a typical WPT or wireless information transmission (WIT) system that utilizes a laser as a source, a high-intensity laser beam must be emitted from a specific distance to the receiver end. A laser-based WPT or WIT usually faces the challenges of mobility and safety; therefore, they typically are used only for low-power and short-distance applications [5]. To overcome the limitations of typical laser-based WPT or WIT systems, the OWIPT system in this study enabled high-power beam transmission through a laser resonant cavity. This RBC-based OWIPT system utilized a resonant beam to transmit watt-level power over meter-level ranges and to multiple mobile devices concurrently. In the case that any obstacle blocks the beam, the resonant beam path stops the resonance mechanism immediately. When any obstacle is in the transmission path, diffraction loss in the cavity increases. Then, if the diffraction loss becomes larger than the system gain produced by the gain medium, the resonance terminates instantly. Conversely, when the obstacle moves out of the transmission path, the loss becomes smaller than the gain factor; therefore, the resonance is immediately reconstituted."

Comment 2:

Figure 5 and Figure 6 can be clearer. The words are too small, and B image in the Figure 5 can not be seen clearly. It is recommended to draw 5 with different color lines (do not use black lines).

Response:

Because Figures 5 and 6 were produced by an optical spectrum analyzer, the color lines cannot be changed. However, we have added some additional marks for the wavelength and optical power levels in the Figures 5(a) and 6(a). Conversely, Figures 5(b) and 6(b) were unchanged because they are only noise-level spectra.

Comment 3:

The author's English expression ability needs to be improved. It is recommended that more conjunctions be used to make the sentence more smooth when comparing the two pictures.

Response:

Thank you for reviewing our manuscript thoroughly. The revised manuscript has been edited for proper English grammar, word usage, and overall style by a native English-speaking academic editor. Furthermore, we have added suitable conjunctions in the description of each picture.

Wallace Academic Editing

English Editing Certificate

This certifies that the paper **Implementation of a Fiber-Based Resonant Beam System for Multiuser Optical Wireless Information and Power Transfer** has been edited by Romanowski Richard on July 7, 2020 and is considered to be improved in grammar, punctuation, spelling, verb usage, sentence structure, conciseness, general readability, writing style, and native English usage to the best of the editor's ability.

Best regards,
Wallace Academic Editing

Phone No.: +886-2-2555-5830
Website: http://www.editing.tw
Email: editing@editing.tw
Address: 3F., No.180, Chang'an W. Rd., Datong Dist., Taipei City

Highlights

- Resonant beam system for simultaneous optical wireless information and power transfer.
- Method of fiber-based with all-fiber components for resonant beam effect.
- Built-in safety mechanism for optical wireless information and power transfer.
- Multi-User optical wireless information and power transfer.

Implementation of a Fiber-Based Resonant Beam System for Multiuser Optical Wireless Information and Power Transfer

Chun-Ming Huang[a], Eddy Wijanto[b], Shin-Pin Tseng[c], Yu-Hao Liu[b], Yu-Tang Luo[b], Hui-Chi Lin[b] and Hsu-Chih Cheng[b*]

[a] Department of Electronic Engineering, National Formosa University, Yunlin County 63201, Taiwan, R.O.C.
[b] Department of Electro-Optical Engineering, National Formosa University, Yunlin County 63201, Taiwan, R.O.C.
[c] Department of Electronic Engineering, National United University, Miaoli County 36003, Taiwan, R.O.C.

Abstract. A fiber-based resonant beam system is proposed for a simultaneous optical wireless information and power transfer (OWIPT) system. A fiber Bragg grating and an optical circulator are used to achieve simultaneous wireless optical communication and power transmission. In the receiver subsystem, a communication and energy harvesting circuit is employed to separate alternating current (AC) and direct current (DC) outputs. The AC output is used for information transmission, and the DC output is used for power transfer. We conducted experiments to test the built-in safety mechanism to verify whether the resonant beam stops immediately if any obstacle obstructs the line of sight of the system. The proposed architecture can be constructed for indoor and outdoor multiuser applications. The results demonstrated that the proposed fiber-based resonant beam system can be implemented successfully for simultaneous OWIPT.

Keywords: Resonant beam, free-space optics, energy harvesting, optical wireless information and power transfer.

***Corresponding author *E-mail address*: chenghc@nfu.edu.tw

1 Introduction

Smartphones and other mobile devices have become an inseparable part of today's daily lives. Throughout the day, most people are sending messages and emails, making voice or video calls, posting on social networks, and playing online games. The increasing usage of mobile devices also increases the average daily power consumption from a typical device battery. In addition, fifth-generation (5G) mobile technologies are projected to support massive amounts of data at high bit rates with minimal delay [1]. This feature of 5G technologies will stimulate many new applications with sophisticated multimedia signal processing, which will increase battery usage.

Furthermore, rapid development of the Internet of things (IoT) is driving the demand for high-bit-rate and low-latency wireless information transfer. One challenge of the IoT is that typical IoT

devices are designed to operate from battery power and have limited energy. Some IoT devices cannot have their batteries replaced. In addition, frequent battery charging for mobile devices by using conventional wired mechanisms tends to obstruct user mobility. In such cases, wireless power transmission (WPT) can be a solution. Free-space optics (FSO) is a promising WPT method [2] that provides high data rates, is immune to radio frequency (RF) interference, does not require licensing, provides a highly secure communication link, is relatively fast, and can be deployed easily. The only substantial consideration for FSO is line of sight (LOS) between the transmitter and receiver.

Simultaneous wireless information and power transfer (SWIPT) technology simultaneously transmits information signals and energy through air [3,4]. SWIPT can strike a balance between message transmission rate and energy harvesting [5]. Because of the superiority of optical systems, optical wireless power transfer (OWPT) has been investigated [6–11]. With traditional OWPT technology, it is challenging to provide watt-level power transmission across meter-level distances for IoT and mobile applications [12,13]. Distributed laser charging (DLC) may offer a wireless power solution for these problems. In DLC systems, photons are amplified regardless of their angle of incidence as long as they travel along the LOS between two retroreflectors. Hence, the intracavity laser generated by a DLC resonator can be self-aligned without the need for specific positioning or tracking. The maximum power transfer efficiency depends on the transmitter input power, laser wavelength, transmission distance, and photovoltaic (PV) cell temperature. SWIPT is possible as long as the communication and network modules are integrated into the DLC transmitter and receiver [14]. A DLC system is safe because its laser can be stopped immediately when any obstacle stands athwart the LOS. When designing any DLC system for maximal power

transmission efficiency, the effects of laser wavelength, transmission attenuation, and PV cell temperature should be evaluated [15].

Light-wave power transfer can be combined with RF power transfer to utilize the bands of both transmission resources in their entirety [16]. A hybrid system can be implemented to solve the LOS consideration in light-wave power transfer and to solve the safety aspect of RF power transfer. With suitable combination protocols, a hybrid system of this type can be used to overcome the challenges of each technology and elevate the overall performance gain.

In simultaneous light-wave information and power transfer for visible light or infrared communication systems with a simple solar panel at the receiver, adjustment strategies can be deployed to balance the trade-off between the harvested energy and quality of service [17]. Such strategies include making separate adjustments to transmission and reception and coordinated adjustments to transmission and reception. With careful adjustments, the maximum harvested energy, information rate, and signal-to-noise plus interference ratio can be optimized.

Various optical wireless information and power transmission (OWIPT) systems based on resonant light have been demonstrated in several experiments [5,18,19]. In this type of system, a gain medium is placed between the transmitting and receiving ends of the module. Light bounces off the mirror; as the light oscillates back and forth, the system develops resonant light. A resonant beam charging (RBC) system can transmit wireless power from a transmitter to a receiver through a resonant beam. A typical RBC system includes a current regulator, diode pump, gain medium, two retroreflectors—R_1 and R_2, and a PV panel [5]. Figure 1 illustrates the features of an OWIPT system based on a resonant beam. In a typical WPT or wireless information transmission (WIT) system that utilizes a laser as a source, a high-intensity laser beam must be emitted from a specific distance to the receiver end. A laser-based WPT or WIT usually faces the challenges of mobility

and safety; therefore, they typically are used only for low-power and short-distance applications [5]. To overcome the limitations of typical laser-based WPT or WIT systems, the OWIPT system in this study enabled high-power beam transmission through a laser resonant cavity. This RBC-based OWIPT system utilized a resonant beam to transmit watt-level power over meter-level ranges and to multiple mobile devices concurrently. In the case that any obstacle blocks the beam, the resonant beam path stops the resonance mechanism immediately. When any obstacle is in the transmission path, diffraction loss in the cavity increases. Then, if the diffraction loss becomes larger than the system gain produced by the gain medium, the resonance terminates instantly. Conversely, when the obstacle moves out of the transmission path, the loss becomes smaller than the gain factor; therefore, the resonance is immediately reconstituted.

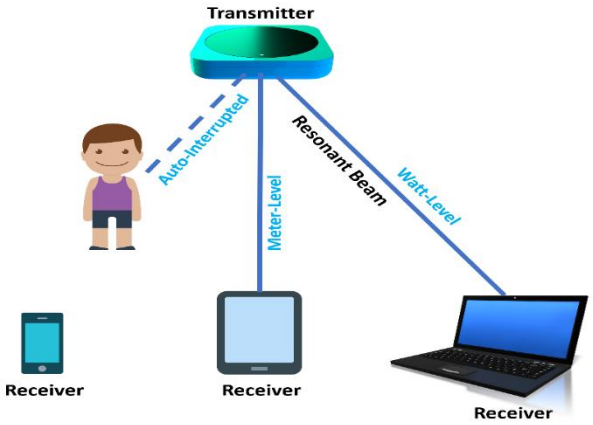

Fig. 1. Features of OWIPT.

Another method to realize a resonant beam mechanism was developed using diverging angular dispersion and spatially distributed laser cavity resonance [18]. A diffraction grating was used to disperse broadband light, and the field of view was expanded using a telescope. To realize the self-alignment feature, retroreflectors reflected the incident beam to complete the resonant beam mechanism. As a built-in safety mechanism, when any vulnerable organ obstructs the LOS of this OWIPT system, the resonance beam is stopped.

The design of the OWIPT receiver plays a crucial role in increasing the efficiency of the system in terms of receiving power. An optical wireless communication receiver that uses a solar panel as a photodetector was proposed in [19]. This system supported simultaneous data transmission and power transfer. Solar panels were used to convert modulated optical signals into electrical signals without the use of any external power. Energy was harvested from the direct current (DC) output of the modulated light; the information signal was obtained from the alternating current (AC) output by using orthogonal frequency-division multiplexing as the signature code.

In the present study, we developed a fiber-based resonant beam system for OWIPT. The resonant beam effect was produced by using all-fiber components. We conducted experiments in both uninterrupted and interrupted scenarios. The interrupted scenario demonstrated the safety mechanism of the proposed system. The all-fiber system is beneficial for far-field OWIPT applications because it is free of electromagnetic interference and does not affect existing radio communications. The system architecture and implementation of the proposed fiber-based resonant beam system for single and multiple users are explained in this paper.

The remainder of this paper is organized as follows. Section 2 introduces the proposed fiber-based OWIPT system, including the system architecture, the derivation of optical power transmission, and the multiuser scheme. Section 3 presents the experimental results for single-user and multiuser fiber-based OWIPT systems in both uninterrupted and interrupted scenarios. Finally, our conclusions are presented in Section 4.

2 Proposed Fiber-Based OWIPT System

The working principle of the proposed fiber-based OWIPT system is based on the RBC system. Two fiber Bragg gratings (FBGs) of the same central wavelength (λ_1) are used to generate

resonant light for the RBC. In the transmitter subsystem, an erbium-doped fiber amplifier (EDFA) that provides a stable 980-nm laser is used as the pumped source for wavelength division multiplexing (WDM). After the optical signals from the EDFA-pumped laser source pass through the WDM and isolator, they are received by an erbium-doped fiber (EDF) that amplifies and converts the signals into the 1550-nm band. The isolator is used to prevent the incidence of unwanted feedback light. From the EDF, the optical signals then pass through the optical circulator, which separates the optical signals traveling in opposite directions. An optical coupler is used to split these optical signals into two output sources, 1% for optical power monitoring and 99% for transmission into free space. The specified wavelength from FBG is then reflected back to the circulator to complete the resonance effect. For information transmission, an electro-optical modulator (EOM) is used to modulate the optical signals. The construction of the proposed fiber-based OWIPT is detailed in Figure 2.

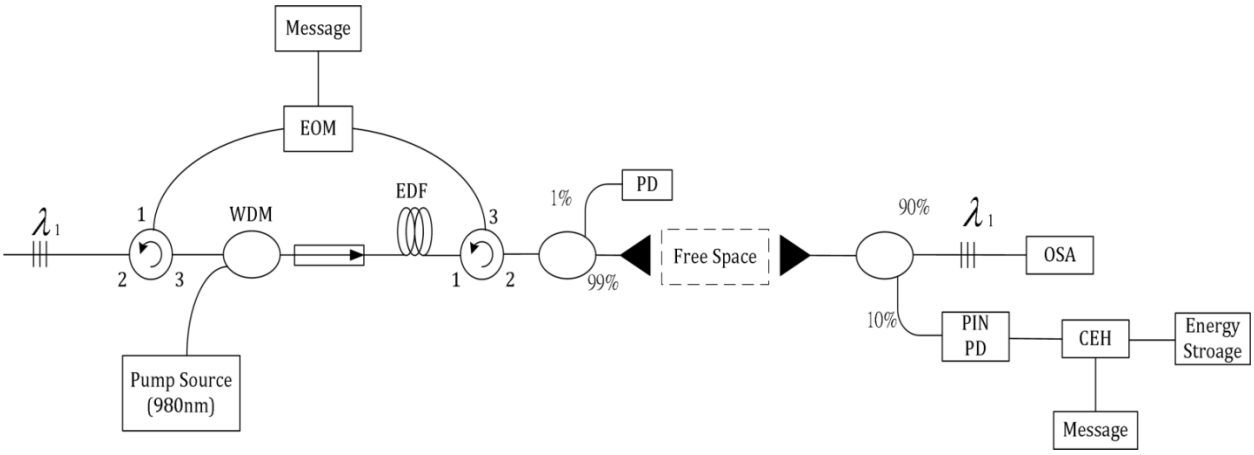

Fig. 2. Fiber-based OWIPT architecture.

In the receiver subsystem, the photodetector (PD) receives light and converts it into electrical signals. The AC and DC elements of the received signal are separated using a communication and energy harvesting (CEH) circuit to complete the process of DC power storage and AC signal transmission. Power storage is expressed in terms of DC current (I_{DC}) and DC voltage (V_{DC})

measured at the DC part. The CEH equivalent circuit is illustrated in Fig. 3. In the experiment, L_0 = 50 mH, C_0 = 330 μF, R_L = 0.6 Ω, and R_C = 470 Ω were used.

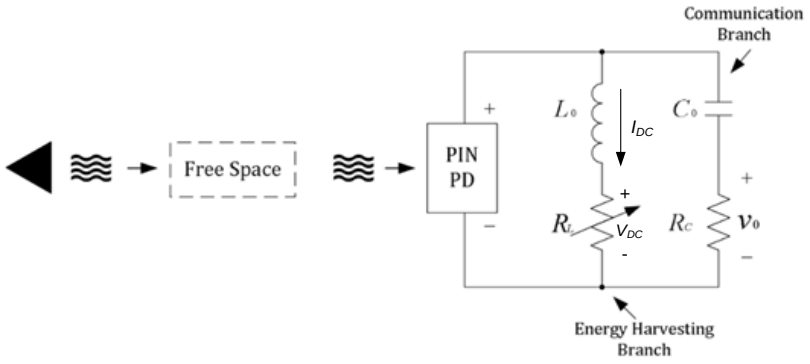

Fig. 3. CEH equivalent circuit.

Optical power transmission based on fiber-optic resonant beam transmission technology can be divided into three stages, namely pumping laser power (P_{pump}) formed by input current, receiving laser output power (P_{laser}), and PD output power after photoelectric conversion ($P_{pv,o}$). The function of P_{pump} as input current I_{in} can be expressed as follows [5]:

$$P_{pump}\left(I_{in}\right)=\frac{hC}{q\lambda}\eta_e\left[I_{in}-I_{th}\right] \tag{1}$$

where h is Planck's constant, C is the speed of light in vacuum, q is the electron charge, λ is the operating wavelength, η_e is the external quantum efficiency, and I_{th} is the critical current. The laser output power P_{laser} at the receiving end can be computed as follows [5]:

$$P_{laser}=\eta_{store}P_{pump}f\left(d\right)+C \tag{2}$$

where η_{store} is the conversion efficiency of population reversal, $f\left(d\right)$ is a function of the internal parameters, where d is the distance between two terminals, and C is a constant value depending on the internal parameters.

The current–voltage (I–V) characteristics of the PD can be computed as follows [5]:

$$I_{pv,o} = I_{ph} - I_d - \frac{V_d}{R_{sh}} \tag{3}$$

$$I_d = I_0 \left(e^{\frac{V_d}{n_s n V_T}} - 1 \right) \tag{4}$$

$$V_d = V_{pv,o} + I_{pv,o} R_s \tag{5}$$

where I_0 is the reverse saturation current, n_s is the number of PDs in series, n is the diode ideal factor, $V_T = \frac{kT}{q}$ is the junction thermal voltage of the diode, k is the Boltzmann constant, and T is the temperature (K). Given the input optical power $P_{pv,i}$ of the PD, the photogenerated current I_{ph} can be written as follows [5]:

$$I_{ph} = \rho P_{pv,i} \tag{6}$$

where ρ is the responsivity (A/W) of the photoelectric conversion. Equation (6) can be used to prove the linear relationship between the photogenerated current (I_{ph}) and the input optical power ($P_{pv,i}$).

If the temperature changes slowly, η_e can be assumed to be constant, and the distance d in $f(d)$ can be assumed to be constant attenuation, η_d, at a certain distance. The output current of the PD can be operated in a linear range according to the following formula [5]:

$$I_{pv,o} \approx I_{ph} = \rho \left\{ \eta_{store} \eta_d \left\{ \frac{hC}{q\lambda} \eta_e \left[I_{in} - I_{th} \right] \right\} + C \right\} = \gamma \left[I_{in} - I_{th} \right] + \beta \tag{7}$$

$$\gamma = \rho \eta_{store} \eta_d \eta_e \frac{hC}{q\lambda} \tag{8}$$

$$\beta = \rho C \tag{9}$$

where both γ and β are constants. This demonstrates the linear modulation of wireless optical information systems based on resonant beams.

Expanded experiments can involve multiuser OWIPT schemes, which can allow users in different bands to use fiber-based RBC architectures. Figure 4 illustrates an architecture for two users. For more than two users, this architecture can be expanded by following the same principle.

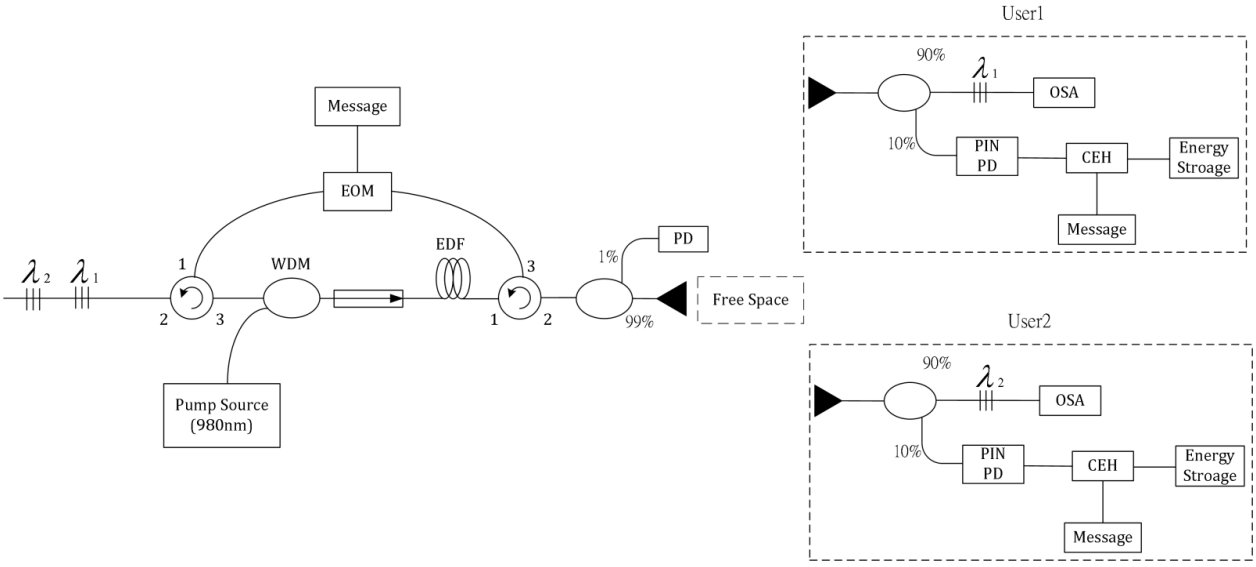

Fig. 4. Multiuser fiber-based OWIPT architecture.

In the transmitter, two FBGs (λ_1 and λ_2) reflect different users' optical signals. Because the transmitter is paired with one or more receivers, each user utilizes one pair of FBGs with the same wavelength for resonating. In the experiment, two pairs of FBGs with different wavelengths (λ_1 and λ_2) were used for user #1 and user #2, respectively. In the receiver, an FBG of the corresponding wavelength is used to split the signals across users. The optical signals are divided into two branches. The first branch is used to reflect the signals back into the circulator, thus completing the resonant beam scheme. The second branch is used for information and power harvesting. The reflected optical signal enters the EOM and is modulated using a signal generator for information transmission. In this experiment, the information sent from the message part to the EOM is a broadcast message from one transmitter to two receivers.

3 Experimental Results

The purpose of the first experiment was to verify the feasibility of the proposed fiber-based resonant beam OWIPT. To this end, we first conducted an experiment to determine whether the OWIPT system signal had the desired resonance effect. In this experiment, EDFA was used to provide a stable 980-nm pumped laser source. The EDF received the EDFA-pumped laser source signal and converted it into a 1550-nm band source signal. Uniform FBGs (Reflectivity 99%, 3L Technologies Inc., Taiwan) with central wavelengths of 1546 nm ($\lambda 1$) and 1549 nm (λ_2) were used to realize the resonance effect. A collimator was used to align the light such that it was transmitted as a parallel light output. Optical couplers (Fiber Optic Communications, Inc., Taiwan) were used as 1 × 2 splitters, and a 10-Gb/s integrated optic intensity modulator (Pirelli, Italy) was used to modulate the signal of the pattern output. A 33120A pulse pattern generator (Hewlett Packard, United States) was used to generate the desired patterns for information transmission. A single-mode circulator (1550 nm and 500 mW; FCIR-1550-3-3-A-0-1-2-1-2) was used as the optical circulator, and a PD with ±15 V constant voltage–current limiting power supply (model-1601, New Focus, California) was used to convert the optical signals into electrical signals. A 2-mm InGaAs PIN photodetector (PIN PD) was used to receive and forward the electrical signal into the CEH circuit. An oscilloscope (OSC, TDS2102B, Tektronix, Oregon, United States) was used to monitor the PD outputs, and an optical spectrum analyzer (MS9710C, Anritsu, Japan) was employed to assess the accuracy of the spectral output. The range of free space in this experiment was 10 cm. The component specifications of the CEH circuit are summarized in Table 1.

The output of the optical coupler was the first detection point at the transmission end, and it was used for optical power monitoring. The second detection point was the transmission end of the FBG, and it was used to detect whether a resonant beam had been produced.

Table 1 Component specifications of the CEH circuit.

Component	L_0	C_0	R_L	R_C
Specification	50mH	330μF	0.6Ω	470Ω

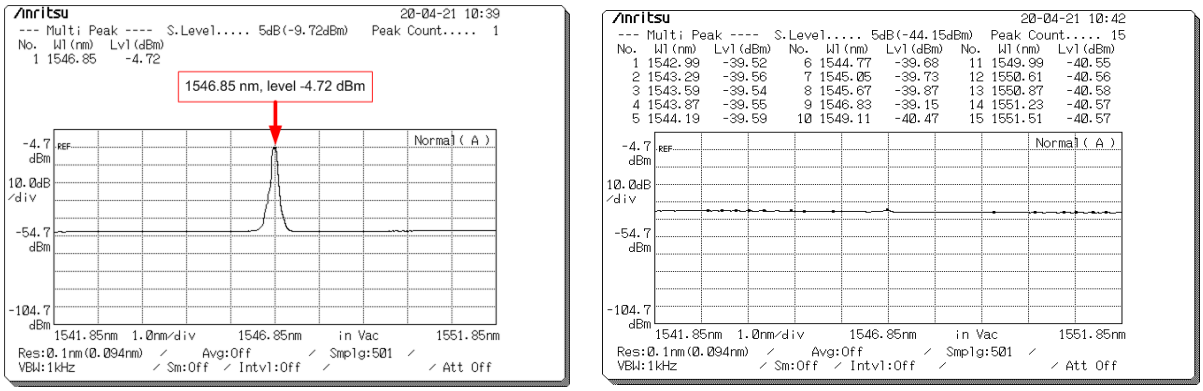

(a) (b)

Fig. 5. Spectrum of λ_1 at the first detection point in the (a) uninterrupted scenario and (b) interrupted scenario.

First, we conducted experiments for the single-user scheme. Figure 5 depicts the spectrum of λ_1 recorded at the first detection point. Figure 5(a) illustrates the spectrum of λ_1 without interruption, where the light intensity is approximately −4.72 dBm while Figure 5(b) shows the spectrum after interruption. This figure indicates no resonance effect at this time. No significant spectrum was detected; only a noise-level spectrum was produced from the reflection wavelength of the FBG at the transmission end.

Figure 6 shows the spectrum of λ_1 recorded at the second detection point. Figure 6(a) depicts the spectrum without interruption, where the light intensity is −0.32 dBm. After the light passes through free space, the light's power is attenuated. Furthermore, Figure 6(b) depicts the spectrum after interruption when only a noise-level signal was left, indicating that the signal and the resonant

light had not been received. These results prove that the system is safe for users because in the presence of an obstacle, no power is received.

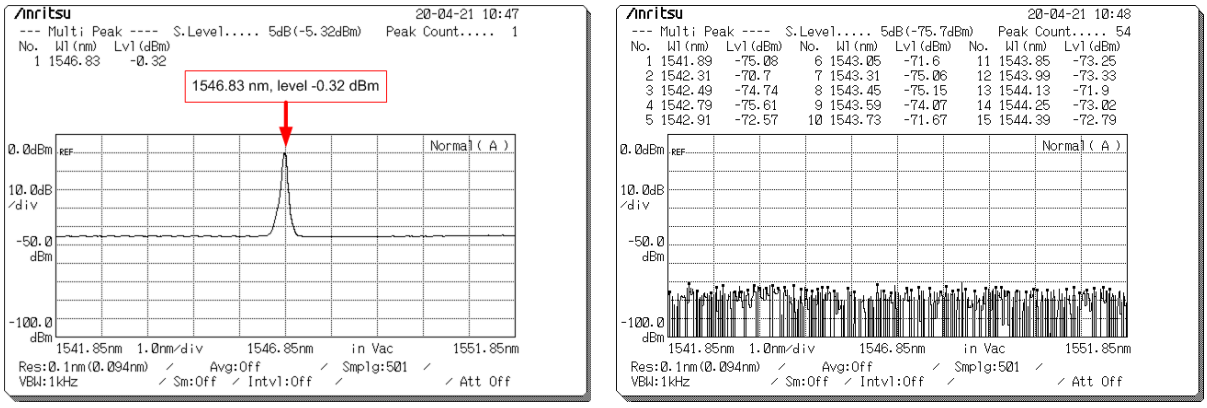

(a) (b)

Fig. 6. Spectrum of λ_1 at the second detection point in the (a) uninterrupted scenario and (b) interrupted scenario.

To verify the resonance effect in the fiber loop, the signals from the detection point were observed at several EOM frequencies. Figure 7 presents the waveform of λ_1 at the first detection point for various frequencies. First of all, Figure 7(a) illustrates the waveform for the EOM frequency of 100 kHz. The resonant waveform (CH#1) and the reference waveform (CH#2) have the same frequencies, indicating that the EOM successfully modulated the optical signals in the fiber loop. The peak-to-peak voltages of the resonant waveform and reference waveform are 83.8 and 75.2 mV, respectively. Subsequently, Figure 7(b) shows the waveform for the EOM frequency of 10 MHz. The same frequency is produced by CH#1 and CH#2, thus proving that the optical signals are successfully modulated by EOM in the fiber loop. The peak-to-peak voltage of the resonant waveform and reference waveform are 73.3 and 55.3 mV, respectively. Afterwards, Figure 7(c) demonstrates the waveform corresponding to the EOM frequency of 15 MHz. The frequencies measured at CH#1 and CH#2 are identical, indicating that the EOM completely

modulated the optical signals in the fiber loop. The peak-to-peak voltages of the resonant waveform and reference waveform are 71.7 and 33.3 mV, respectively.

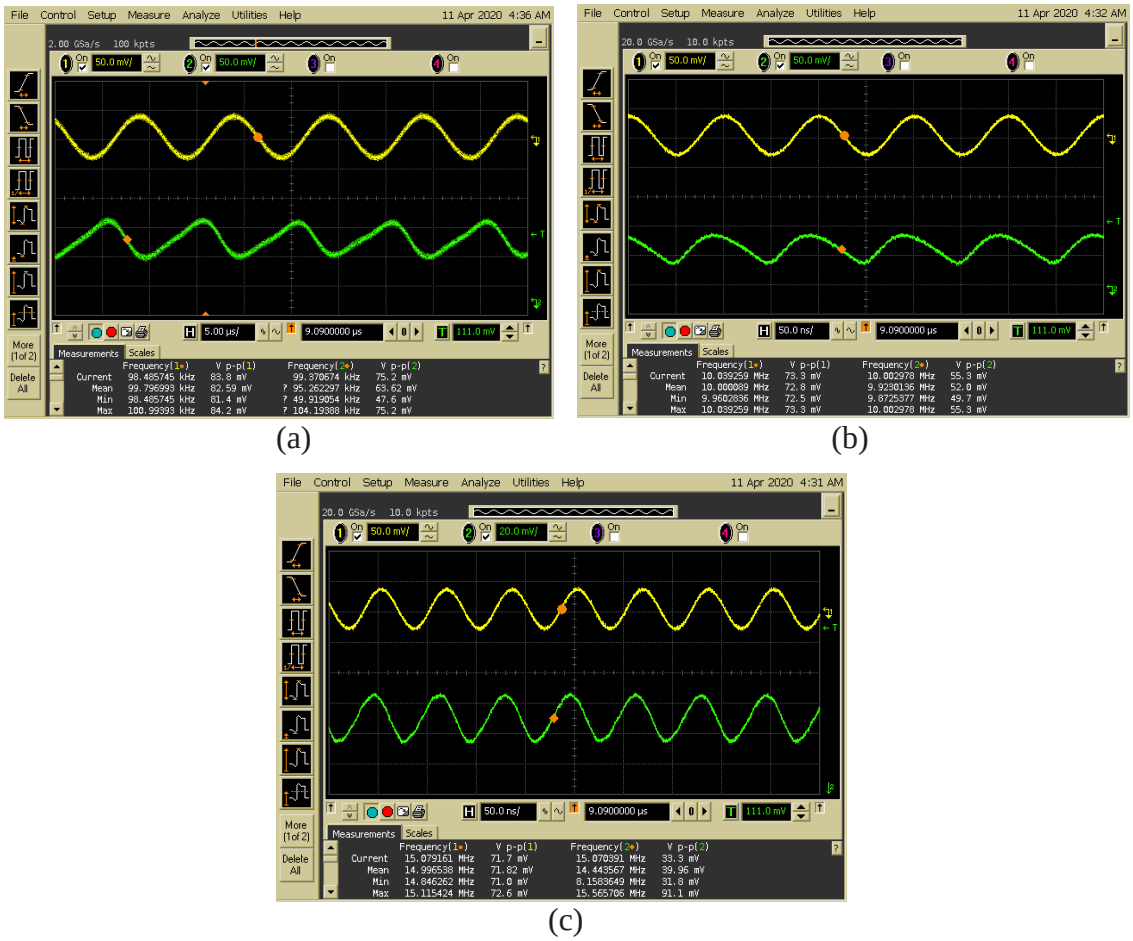

Fig. 7. Waveform of λ_1 at the first detection point for the signal frequencies of (a) 100 kHz, (b) 10 MHz, and (c) 15 MHz.

Because bit rate affects system performance, we observed the waveforms at the detection points under different bit rates. Figure 8 illustrates the waveform of λ_1 at the first detection point under different bit rates.

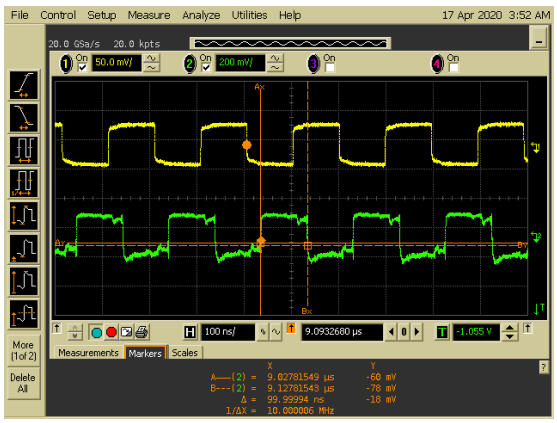

(a)

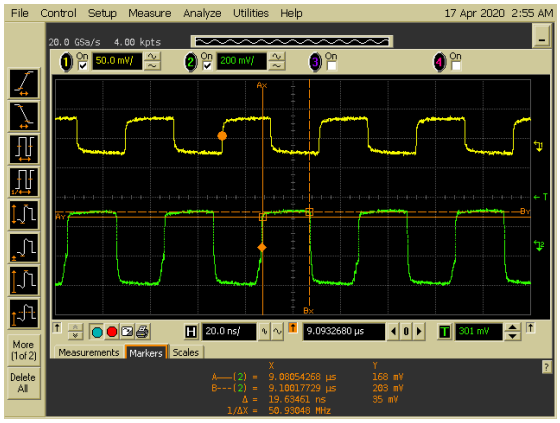

(b)

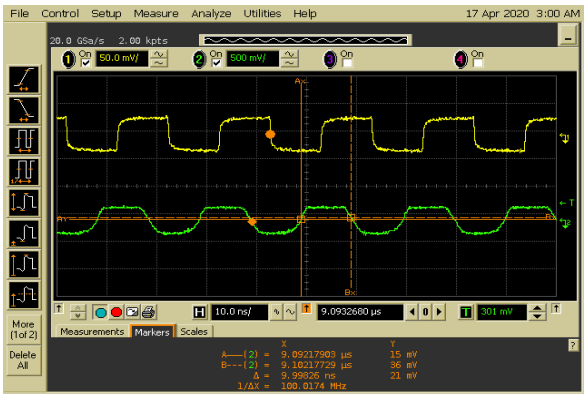

(c)

Fig. 8. Waveform of λ_1 at the first detection point under the bit rates of (a) 10 Mbps, (b) 50 Mbps, and (c) 100 Mbps.

Firstly, Figure 8(a) displays the waveform under the bit rate of 10 Mbps. CH#1 and CH#2 have the same frequency, indicating successful modulation of the optical signals by the EOM in the fiber loop. The voltage difference is −18 mV. Next, Figure 8(b) graphs the waveform corresponding to the bit rate of 50 Mbps. CH#1 and CH#2 have the same frequency, which indicates that the EOM successfully modulated the optical signals in the fiber loop. The voltage difference is 35 mV. After that, Figure 8(c) illustrates the waveform under the bit rate of 100 Mbps.

CH#1 and CH#2 have the same frequency, thus indicating that the EOM successfully modulated the optical signals in the fiber loop. The voltage difference is 21 mV.

Next, the waveforms of the CEH subsystem were observed to monitor the performance of the proposed system. Figure 9 shows the waveform of λ_1 originating from the *Rc* in the CEH circuit.

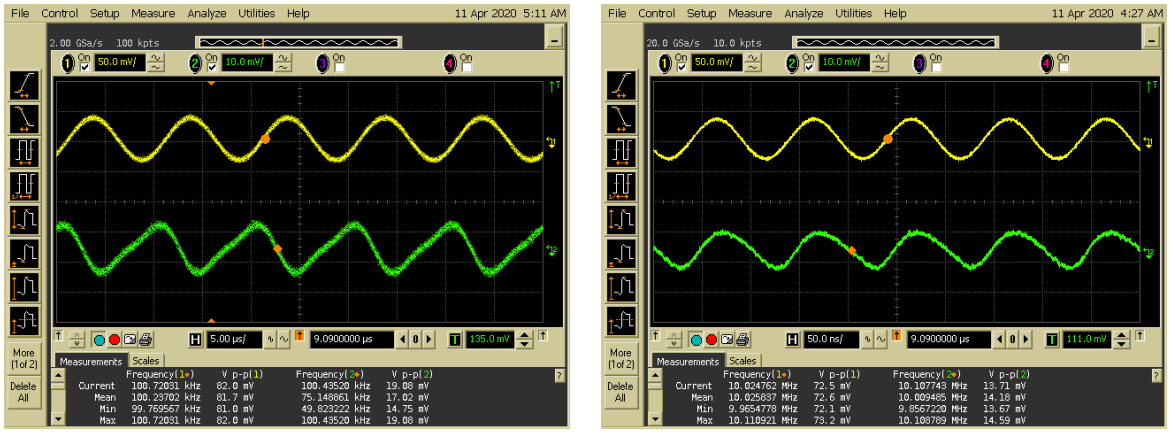

(a) (b)

(c)

Fig. 9. Waveform of λ_1 originating from *Rc* in the CEH circuit under the signal frequencies of (a) 100 kHz, (b) 10 MHz, and (c) 15 MHz.

Initially, Figure 9(a) shows the waveform obtained with the EOM frequency of 100 kHz. CH#1 and CH#2 have the same frequency, thus indicating complete modulation of the optical signals by the EOM in the fiber loop. The peak-to-peak voltages of the resonant waveform and reference waveform are 82 and 19.08 mV, respectively. Further, Figure 9(b) plots the waveform obtained

with the EOM frequency of 10 MHz. CH#1 and CH#2 have the same frequency, thus indicating successful modulation of the optical signals in the fiber loop by the EOM. The peak-to-peak voltages of the resonant waveform and reference waveform are 72.5 and 13.71 mV, respectively. Lattermost, Figure 9(c) displays the waveform obtained with the EOM frequency of 15 MHz. CH#1 and CH#2 have the same frequency, thus verifying successful modulation of the optical signals. The peak-to-peak voltages of the resonant waveform and reference waveform are 70.6 and 8.78 mV, respectively.

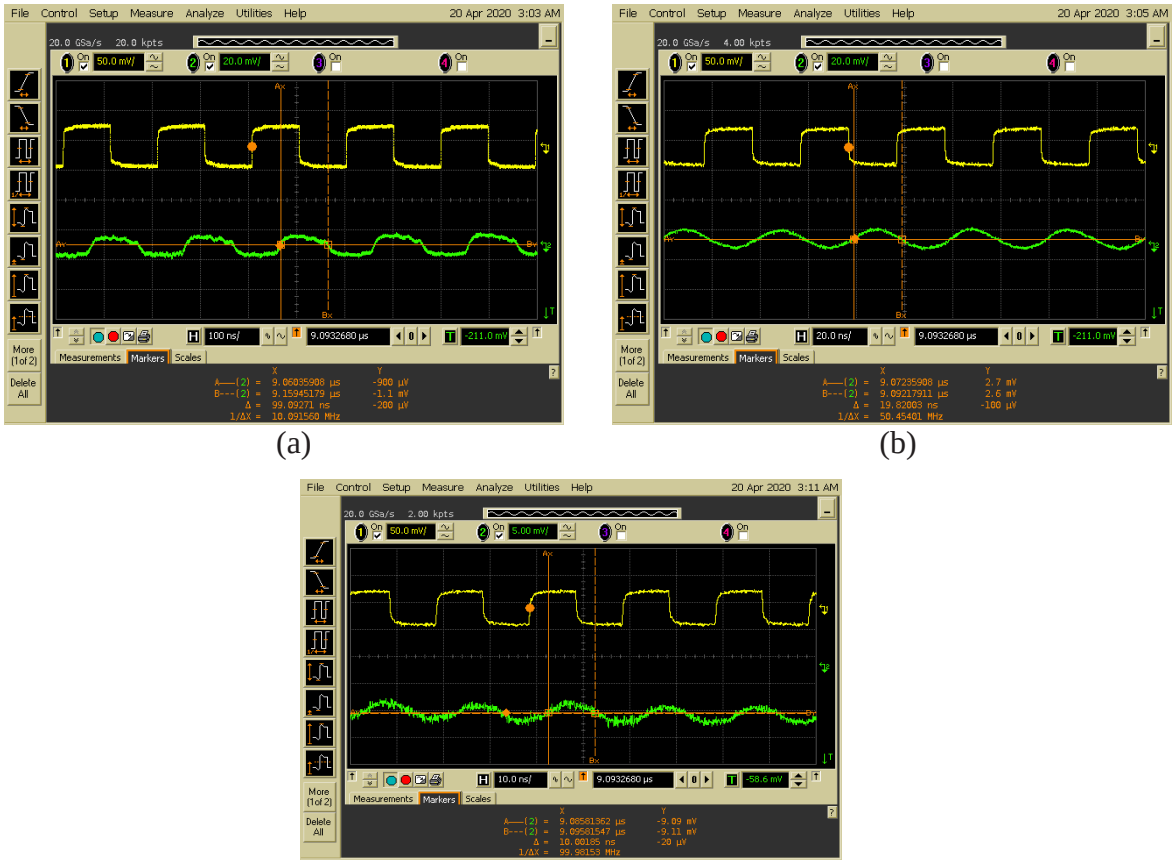

(a) (b)

(c)

Fig. 10. Waveform of λ_1 originating from *Rc* in the CEH circuit under the bit rates of (a) 10 Mbps, (b) 50 Mbps, and (c) 100 Mbps.

The waveforms originating from the CEH subsystem under different bit rates were measured for the single-user scheme. Figure 10 presents the waveform of λ_1 originating from *Rc* in the CEH circuit under different bit rates. Figure 10(a) presents the waveform under the bit rate of 10 Mbps. CH#1 and CH#2 have the same frequency, indicating complete modulation of optical signals in the fiber loop. The voltage difference is -200 μV. Then, Figure 10(b) demonstrates the waveform under bit rate of 50 Mbps. CH#1 and CH#2 have the same frequency, thus proving modulation of optical signals in the fiber loop. The voltage difference is -100 μV. Afterwards, Figure 10(c) depicts the waveform under the bit rate of 100 Mbps. CH#1 and CH#2 have the same frequency, verifying full modulation of optical signals in the fiber loop. The voltage difference is −20 μV.

Table 2 CEH parameters under different signal frequencies for λ_1.

CEH Parameters	**Frequency**		
	100 kHz	**10 MHz**	**15 MHz**
DC Current	0.99 mA	0.98 mA	0.98 mA
DC Voltage	0.60 mV	0.59 mV	0.59 mV
AC Voltage	82.00 mV_{pp}	72.50 mV_{pp}	70.60 mV_{pp}

Table 3 CEH parameters under different bit rates for λ_1.

CEH Parameters	**Bit Rate**		
	10 Mbps	**50 Mbps**	**100 Mbps**
DC Current	1.05 mA	1.03 mA	1.03 mA
DC Voltage	0.63 mV	0.62 mV	0.62 mV

Tables 2 and 3 summarize the resulting CEH parameters for various frequencies and bit rates, respectively. The DC current and voltage were relatively stable across all frequencies and bit rates.

We conducted a second experiment for the multiuser scheme. When the collimator at the transmitter and the collimator at receiver #2 were aligned, the wavelength of the resonant beam changed from 1546.83 nm (λ_1) to 1549.7 nm (λ_2). Furthermore, the message modulated at the central wavelength of λ_2 from the transmitter could be reconstructed by the FBG of receiver #2 operating at the corresponding wavelength of λ_2.

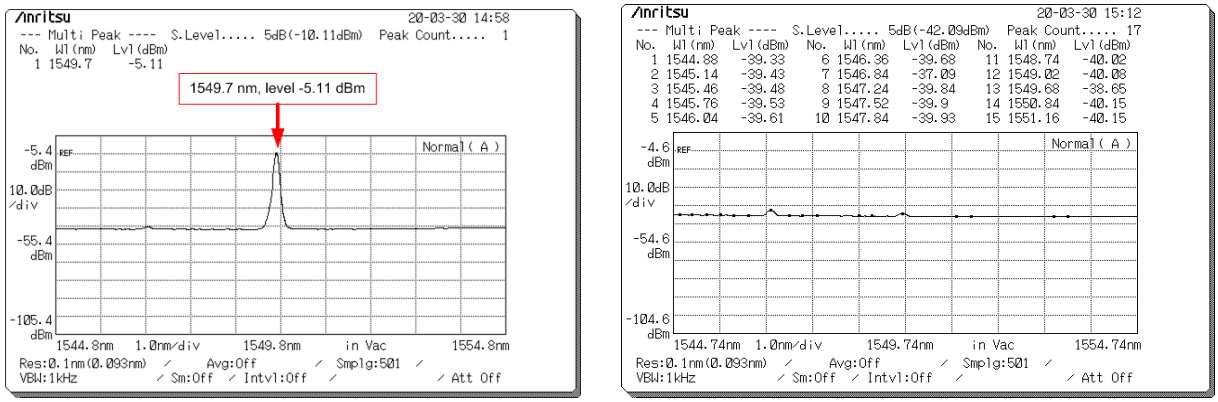

(a) (b)

Fig. 11. Spectrum of λ_2 at the first detection point for (a) uninterrupted scenario and (b) interrupted scenario.

Figure 11 shows the spectrum of λ_2 recorded at the first detection point. First, Figure 11(a) illustrates the spectrum recorded in the scenario without any interruption. The light intensity is approximately −5.11 dBm. In the other hand, Figure 11(b) shows the spectrum recorded after an interruption. No resonance effect exists at this time, and only a small spectrum is produced owing to the reflection wavelength of the FBG at the transmitting end.

Figure 12 demonstrates the spectrum of λ_2 at the second detection point. Initially, Figure 12(a) depicts the spectrum without interruption. The light intensity is −0.87 dBm. The light power is attenuated after passage through free space. Conversely, Figure 12(b) shows the spectrum after

interruption, in which only noise remains. These results demonstrate the effectiveness of the safety mechanism for users in the presence of obstacles along the LOS.

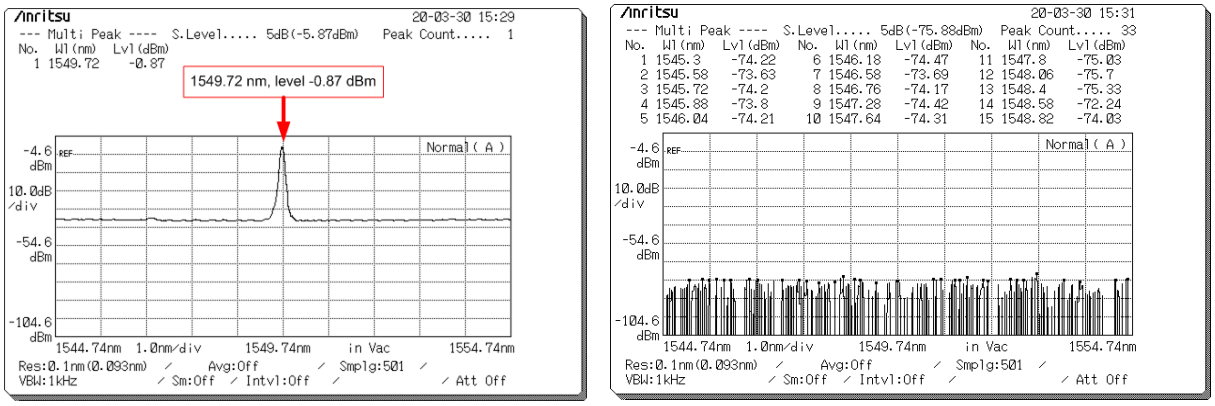

(a) (b)

Fig. 12. Spectrum of λ_2 at the second detection point for (a) uninterrupted scenario and (b) interrupted scenario.

Figure 13 presents the waveforms recorded at the first detection point under different frequencies. First of all, Figure 13(a) illustrates the waveform corresponding to the EOM frequency of 100 kHz. CH#1 and CH#2 have the same frequency, thus verifying complete modulation of the optical signals in the fiber loop. The peak-to-peak voltages of the resonant waveform and reference waveform are 83.9 and 67.7 mV, respectively. Further, Figure 13(b) shows the waveform corresponding to the EOM frequency of 10 MHz. CH#1 and CH#2 have the same frequency, thus indicating full modulation by the EOM in the fiber loop. The peak-to-peak voltages of the resonant waveform and reference waveform are 71.9 and 35.2 mV, respectively. Subsequently, Figure 13(c) demonstrates the waveform corresponding to the EOM frequency of 15 MHz. CH#1 and CH#2 have the same frequency, thus indicating successful modulation of the optical signals in the fiber loop. The peak-to-peak voltages of the resonant waveform and reference waveform are 73.9 and 18.36 mV, respectively.

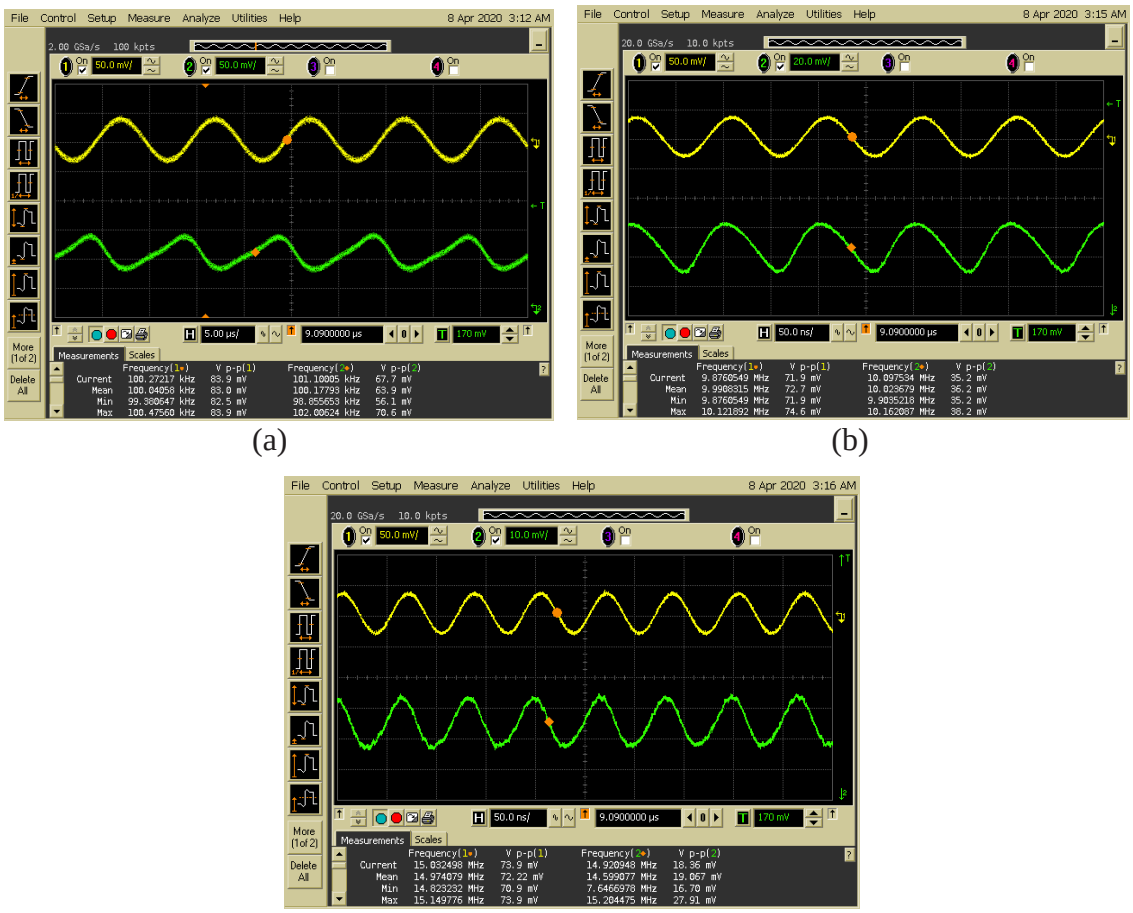

Fig. 13. Waveform of λ_2 at the first detection point under the signal frequencies of (a) 100 kHz, (b) 10 MHz, and (c) 15 MHz.

In a manner similar to that used for the single-user scheme, we tested system performance under different bit rates. Figure 14 shows the waveform of λ_2 at the first detection point under different bit rates. Initially, Figure 14(a) shows the waveform under the bit rate of 10 Mbps. CH#1 and CH#2 have the same frequency, thus verifying complete modulation of the optical signals in the fiber loop. The voltage difference is −3.3 mV. Later, Figure 14(b) shows the waveform under the bit rate of 50 Mbps. CH#1 and CH#2 have the same frequency, thus proving modulation by the EOM in the fiber loop. The voltage difference is 200 µV. At last, Figure 14(c) illustrates the

waveform under the bit rate of 100 Mbps. CH#1 and CH#2 have the same frequency, thus verifying successful modulation of the optical signals in the fiber loop. The voltage difference is −8 mV.

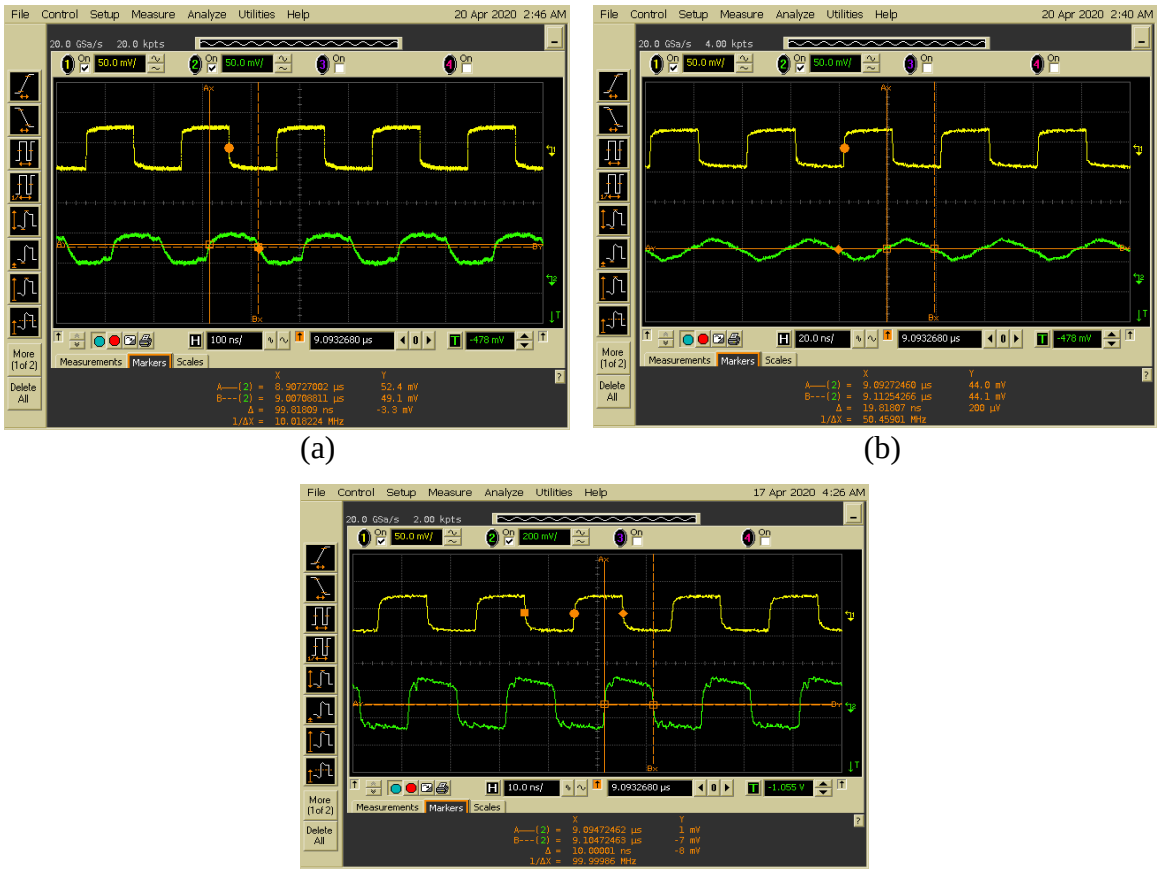

Fig. 14. Waveform of λ_2 at the first detection point under the bit rates of (a) 10 Mbps, (b) 50 Mbps, and (c) 100 Mbps.

The next experiment involved measurement of the CEH circuit. Figure 15 reveals the waveform of λ_2 originating from the *Rc* in the CEH circuit. First, Figure 15(a) shows the waveform corresponding to the EOM frequency of 100 kHz. CH#1 and CH#2 have the same frequency, thus indicating full modulation in the fiber loop. The peak-to-peak voltages of the resonant waveform and reference waveform are 83.3 and 21.9 mV, respectively. Subsequently, Figure 15(b) exhibits the waveform corresponding to the EOM frequency of 10 MHz. CH#1 and CH#2 have the same

frequency, thus verifying complete modulation of the optical signals in the fiber loop. The peak-to-peak voltages of the resonant waveform and reference waveform are 72.9 and 30.1 mV, respectively. Finally, Figure 15(c) displays the waveform corresponding to the EOM frequency of 15 MHz. CH#1 and CH#2 have the same frequency, thus verifying modulation by the EOM in the fiber loop. The peak-to-peak voltages of the resonant waveform and reference waveform are 72.4 and 6.64 mV, respectively.

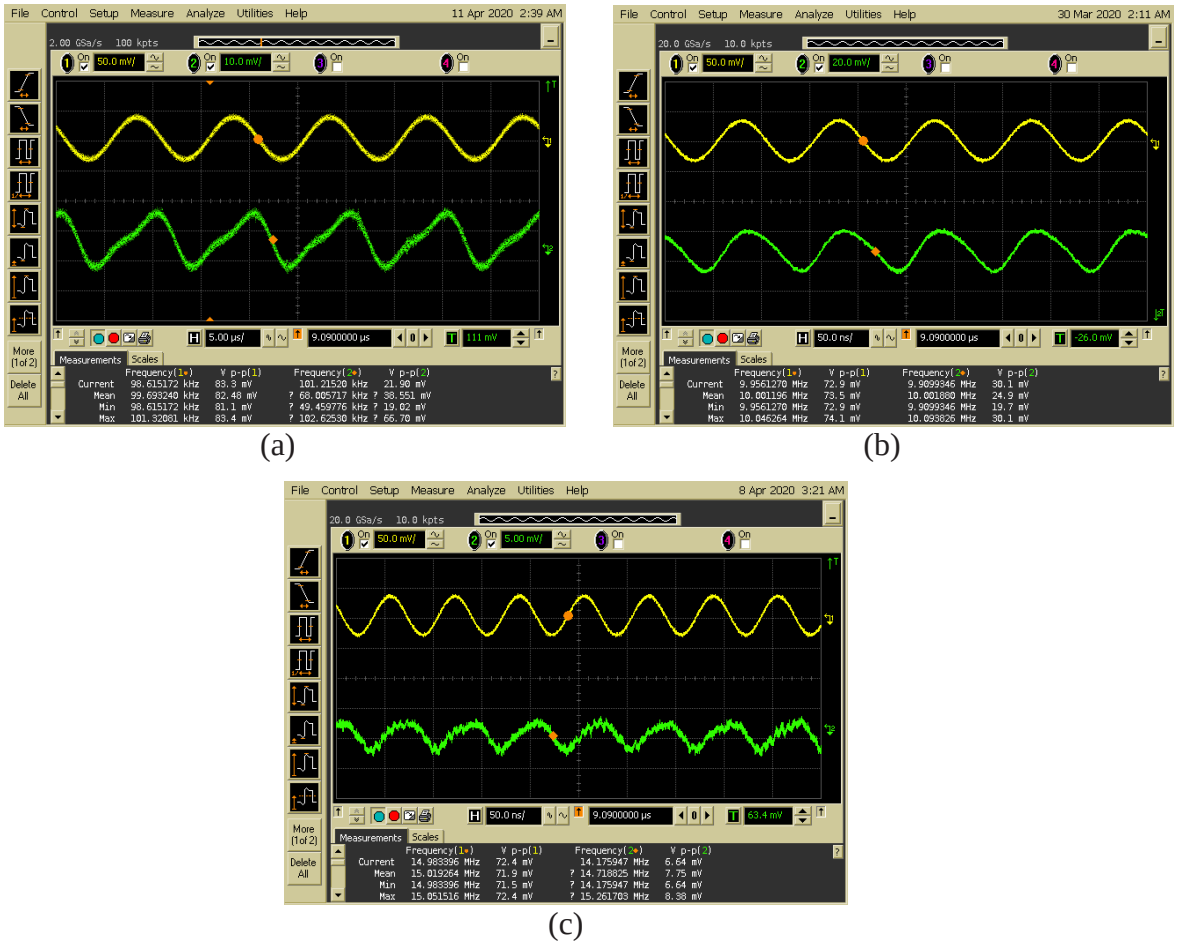

(a) (b)

(c)

Fig. 15. Waveform of λ_2 originating from the *Rc* in the CEH circuit under the signal frequencies of (a) 100 kHz, (b) 10 MHz, and (c) 15 MHz.

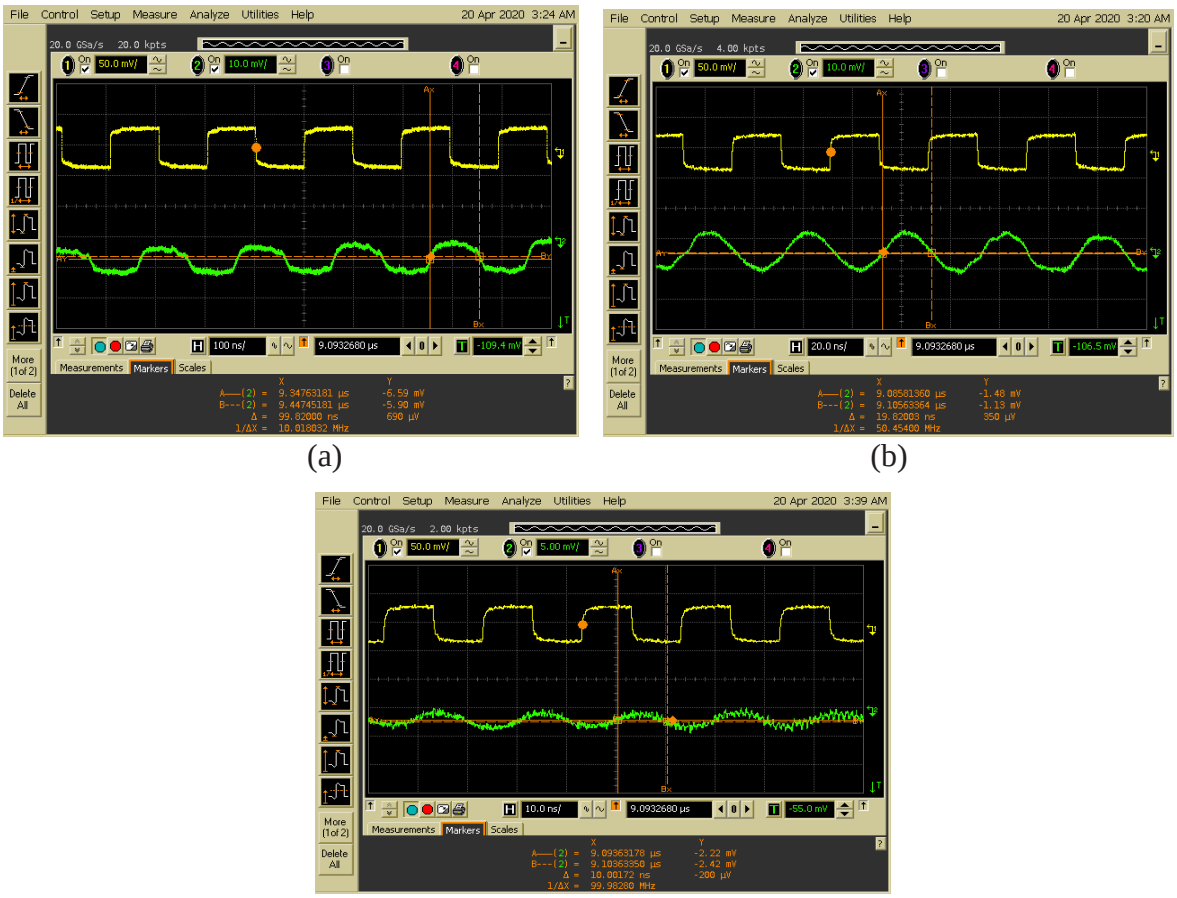

Fig. 16. Waveform of λ_2 originating from the *Rc* in the CEH circuit under the bit rates of (a) 10 Mbps, (b) 50 Mbps, and (c) 100 Mbps.

Figure 16 presents the waveform of λ_2 originating from the *Rc* in the CEH circuit under different bit rates. First of all, Figure 16(a) illustrates the waveform corresponding to the bit rate of 10 Mbps. CH#1 and CH#2 have the same frequency, thus verifying successful EOM modulation of the optical signals in the fiber loop. The voltage difference is 690 µV. Afterwards, Figure 16(b) demonstrates the waveforms corresponding to the bit rate of 50 Mbps. CH#1 and CH#2 have the same frequency, thus indicating complete modulation of the optical signals by the EOM in the fiber loop. The voltage difference is 350 µV. Lattermost, Figure 16(c) shows the waveform corresponding to the bit rate of 100 Mbps. CH#1 and CH#2 have the same frequency, thus

indicating full modulation of the optical signals in the fiber loop. The voltage difference is -200 μV.

Table 4 CEH parameters under different signal frequencies for λ_2.

CEH Parameters	Frequency		
	100 kHz	**10 MHz**	**15 MHz**
DC Current	0.97 mA	0.98 mA	0.99 mA
DC Voltage	0.58 mV	0.59 mV	0.60 mV
AC Voltage	83.30 mV_{pp}	72.90 mV_{pp}	72.40 mV_{pp}

Table 5 CEH parameters under different bit rates for λ_2.

CEH Parameters	Bit Rate		
	10 Mbps	**50 Mbps**	**100 Mbps**
DC Current	0.98 mA	0.97 mA	0.97 mA
DC Voltage	0.59 mV	0.58 mV	0.58 mV

Tables 4 and 5 summarize the CEH parameters for various frequencies and bit rates, respectively. The DC currents and voltage generated by the proposed system were relatively stable across all frequencies and bit rates.

4 Conclusions

A fiber-based resonant beam system was applied to enable simultaneous information and power transmission through free space. Two pairs of FBGs with different wavelengths (λ_1 and λ_2) were used to realize optical resonance and data transmission for multiuser applications. An EOM was used to modulate the optical signals for broadcast information transmission and simultaneously present them in the fiber loop. After the resonance effect had been achieved, some of the optical signals were transmitted to the PIN PD for AC–DC signal separation for power and information

harvesting; the other optical signals were fed back to the fiber loop to complete the resonance effect.

The experiments proved that the power attenuation in the fiber loop was relatively small. More significant power attenuation occurred after the signals passed through free space, where the power dropped by approximately 5 dBm. The power attenuation in free space influenced the photocurrent generated by the PIN PD, resulting in the generation of small DC and AC voltages in the harvesting subsystem. Under the multiuser scheme, the result was approximately 0.55 dBm lower than that under the single-user scheme.

Although power attenuation in free space is a vital consideration that warrants optimization in future research, the experimental results obtained in this study proved that it is possible to use an all-fiber resonant beam system for simultaneous OWIPT.

Acknowledgment

This work was supported by the Ministry of Science and Technology, Taiwan, under Grants MOST 108-2221-E-150-041 and MOST 107-2218-E-150-008-MY2.

References

[1] A. Morgado, A., K.M.S. Huq, S. Mumtaz, J. Rodriguez, A survey of 5G technologies: regulatory, standardization and industrial perspectives, Digit. Commun. Netw. 4 (2018), 87–97.

[2] V. W. S. Chan, Free-Space Optical Communications, J. Lightwave Technol. 24 (2006), 4750-4762.

[3] A. Kurs et al., Wireless Power Transfer via Strongly Coupled Magnetic Resonances, Science. 317 (5834) (2007) 83-86.

[4] P. Sample, D. T. Meyer, and J. R. Smith, Analysis, Experimental Results, and Range Adaptation of Magnetically Coupled Resonators for Wireless Power Transfer, IEEE Trans. Ind. Electron. 58(2) (2011) 544-554.

[5] M. Xiong, Q. Liu, M. Liu, X. Wang and H. Deng, Resonant Beam Communications with Photovoltaic Receiver for Optical Data and Power Transfer, IEEE Trans. Commun. 68(5) (2020) 3033-3041.

[6] D. Killinger, Free Space Optics for Laser Communication Through the Air, Opt. Photon. News, 13 (2002) 36– 42.

[7] K. Sung-Man, R. Dong-Hun, Experimental Demonstration of Optical Wireless Power Transfer with a DC-to-DC Transfer Efficiency of 12.1%, Opt. Eng., 57(8) (2018) 086108.

[8] W. Zhou and K. Jin, Efficiency Evaluation of Laser Diode in Different Driving Modes for Wireless Power Transmission, IEEE Trans. Power Electron., 30 (2015) 6237–6244.

[9] W. J. Wang, and C. Huang, A Coupled Model on Energy Conversion in Laser Power Beaming, J. Power Sources, 393 (2018) 211–216.

[10] H. S. Dhadwal, J. Rastegar, and P. Kwok, Wireless energy and data transfer to munitions using high power laser diodes, in Proc. SPIE 10195, Unmanned Systems Technology XIX, 1019513 (2017).

[11] C. D. Santi, M. Meneghini, A. Caria, E. Dogmus, M. Zegaoui, F. Medjdoub, B. Kalinic, T. Cesca, G. Meneghesso, and E. Zanoni, GaN-Based Laser Wireless Power Transfer System, Materials, 11(1) (2018) 153.

[12] Z. Yuhuan and T. Miyamoto, 200 mW-class LED-based optical wireless power transmission for compact IoT, Jpn. J. Appl. Phy. 58 (2019) SJJC04.

[13] J. Mukherjee et al., Efficiency Limits of Laser Power Converters for Optical Power Transfer Applications, J. Phys. D: Appl. Phys., 46 (2013) 264006.

[14] Q. Liu et al., Charging Unplugged: Will Distributed Laser Charging for Mobile Wireless Power Transfer Work? IEEE Veh. Technol. Mag., 11(4) (2016) 36–45.

[15] Q. Zhang et al., Distributed Laser Charging: A Wireless Power Transfer Approach, IEEE Internet Things J., 5(5) (2018) 3853-3864.

[16] H. Tran, G. Kaddoum, and C. Abou-Rjeily, Collaborative RF and Lightwave Power Transfer for Next-Generation Wireless Networks, IEEE Commun. Mag., 58(2) (2020) 27-33.

[17] G. F. Pan, P. D. Diamantoulakis, Z. Ma, Z. G. Ding, and G. K. Karagiannidis, Simultaneous Lightwave Information and Power Transfer: Policies, Techniques and Future Directions, IEEE Access, 7 (2019) 28250-28257.

[18] J. Lim, T. S. Khwaja, and J. Y. Ha, Wireless optical power transfer system by spatial wavelength division and distributed laser cavity resonance, Opt. Express, 27 (2019) A924-A935.

[19] Z. Wang et al., On the Design of a Solar-Panel Receiver for Optical Wireless Communications With Simultaneous Energy Harvesting, IEEE J. Sel. Areas Commun., 33(8) (2015) 1612-1623.

This piece of the submission is being sent via mail.

Declaration of interests

☒ The authors declare that they have no known competing financial interests or personal relationships that could have appeared to influence the work reported in this paper.

☐The authors declare the following financial interests/personal relationships which may be considered as potential competing interests: